Z. Kristallogr. **2013**, *228*, 629–634 / **DOI** 10.1524/zkri.2013.1686

Liebau density vector: a new approach to characterize lone electron pairs in mullite-type materials

Mariano Curti[I], Thorsten M. Gesing[II], M. Mangir Murshed[II], Thomas Bredow[III] and Cecilia B. Mendive*[,I]

[I] Departamento de Química, Facultad de Ciencias Exactas y Naturales, Universidad Nacional de Mar del Plata, Dean Funes 3350, 7600 Mar del Plata, Argentina
[II] Chemische Kristallographie fester Stoffe, Institut für Anorganische Chemie, Universität Bremen, Leobener Straße NW2, 28359 Bremen, Germany
[III] Mulliken Center for Theoretical Chemistry, Institut für Physikalische und Theoretische Chemie, Universität Bonn, Beringstr. 4, 53115 Bonn, Germany

Received August 9, 2013; accepted October 19, 2013
Published online: November 21, 2013

Lone electron pairs / Wang-Liebau vector / Liebau density vector / Stereochemistry

Abstract. The bismuth $6s^2$ lone electron pair (LEP) in mullite-type $Bi_2M_4O_{9/10}$ (where M = Al, Fe, or Mn) was characterized by means of several parameters derived from experimental and theoretical calculations. The Wang-Liebau eccentricity (WLE) parameter proved to be very useful to quantify the stereochemical activity of the LEPs.

Calculations of electronic distributions (three-dimensional charge density difference isosurfaces) were used as independent measurements, which validated the relevance of the WLE parameter for the characterization and quantification of LEPs. The distribution of the Bi $6s^2$ electrons around the nucleus was evaluated and the maximum of electron density calculated. The spatial orientation of this electron density with respect to the nucleus is expressed as "Liebau density vector". Therefore, this vector is ascribed to be a key result of this work as a proof that the purely geometrically defined Wang-Liebau vector indeed points towards the maximum electron density of the LEP.

The LEP stereochemical activity was studied in terms of the type of structure ($Bi_2M_4O_9$ or $Bi_2M_4O_{10}$) and the nature of M. The effect of exchanging bismuth by lanthanum as well as the relative stabilities of $Bi_2M_4O_9$ or $Bi_2M_4O_{10}$ structures were calculated and discussed.

1. Introduction

The mullite-type O9 compounds with general formula $Bi_2M_4O_9$ (M = Al, Fe) have attracted considerable interest in the last years because of their potential applications in solid oxide fuel cells (SOFCs) [1]. Their main motifs are one-dimensional chains of edge-sharing MO_6 octahedra, interconnected by M_2O_7 double tetrahedral units and BiO_6E groups (E refers to a $6s^2$ lone electron pair, LEP) along the *c*-axis [2] as given in Fig. 1a. The closely related mullite-type O10 structure (*e.g.*, $Bi_2Mn_4O_{10}$) subtly differs from that of O9. Whereas in O9 a single oxygen vertex forms the M_2O_7 double tetrahedra, O10 requires two symmetry equivalent oxygen atoms for the construction of the common edge, forming a M_2O_8 double tetragonal pyramid (Fig. 1b).

In both arrangements there are empty positions between the crystallographically identical bismuth atoms (Fig. 1c and d). In the mullite structure these empty positions (voids) are occupied by additional oxygen atoms [2].

The stereochemistry of LEPs is attributed to the existence of these types of voids, which provide suitable space

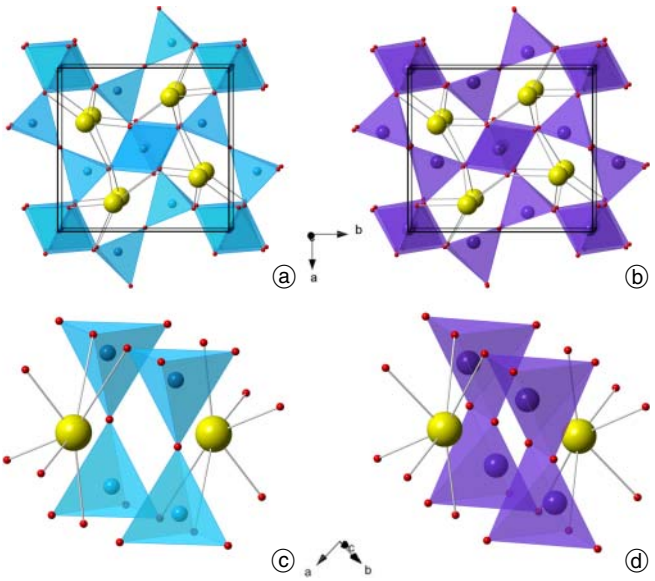

Fig. 1. Experimental structure of mullite-type $Bi_2Al_4O_9$ (**a**) and $Bi_2Mn_4O_{10}$ (**b**) together with the bismuth coordination in $Bi_2Al_4O_9$ (**c**). The void between them allows the lone electron pairs to distribute in a stereochemically active manner. (**d**) Measured bismuth coordination in $Bi_2Mn_4O_{10}$. The "splitting" of oxygen atoms bridging the double tetragonal pyramids leaves much less space for the LEP to be distributed asymmetrically. Yellow spheres represent bismuth atoms, cyan spheres represent aluminum atoms, violet spheres represent manganese atoms, and red spheres represent oxygen atoms.

* Correspondence author (e-mail: cbmendive@mdp.edu.ar)

for an asymmetric distribution of electronic density of the atoms. Abrahams *et al.* [3] proposed that such space in O9 structures could be used by neighboring oxygen atoms as a jump position for a cooperative motion. However, an oxygen jump through this area appears to be unlikely [4] due to the electronic density of the stereochemically active LEPs [5] which causes a high energetic barrier [6].

The jumping mechanism requires some vacancies at the occupied oxygen positions to trigger the cooperative motion. Zha *et al.* [7] reported a relatively high oxygen conductivity of $Bi_2Al_4O_9$ when bismuth was partly replaced with strontium. As a consequence, electro-neutrality requires formation of oxygen vacancies as Bi^{3+} was replaced by Sr^{2+}. If vacancies are created at the required crystallographic sites, the migration may take place as proposed by Abrahams *et al.* [3]. Nevertheless, the samples used for the conductivity measurements were synthesized above 1323 K [7]; at these temperatures, all strontium-doped mullite-type bismuth aluminates are unstable [8]. Under such conditions it is highly probable that the observed high conductivity was due to a thin film of δ-Bi_2O_3 formed around the $Bi_2Al_4O_9$ grains as reported by Ohmann *et al.* [4] who made an extensive comparison between a series of $Bi_2Al_4O_9$ samples synthesized with and without nominal excess of Bi_2O_3 and/or SrO. Recently, Gesing *et al.* [6] provided clear-cut evidences on the incorporation of strontium in $Bi_2Al_4O_9$ samples using multi-quantum ^{27}Al MAS NMR, XPS, XRPD, neutron diffraction, and first-principles calculated charge-density maps. The complimentary techniques supported the hypothesis of a hindered oxygen migration through a region partly shielded by the LEPs. The presence of a LEP and the magnitude of its stereochemical activity are critically important for understanding the crystal chemical properties of these materials. In this report both theoretical and experimental investigations have been aimed to thoroughly characterize the LEPs of the Bi^{3+}/relevant cations within some mullite-type structures.

The Wang-Liebau eccentricity parameter (WLE) was demonstrated to be a useful tool to characterize LEPs of many ions [9–17]. A positive deviation of the structural bond valence sum (BVS) from that of the formal valence [18] have been frequently found for cations with a LEP [14]. The contribution of the LEP to the BVS of the associated ion has been addressed by Wang and Liebau [9], suggesting a vector termed eccentricity parameter $\boldsymbol{\Phi}_i$. The direction of $\boldsymbol{\Phi}_i$ is considered along the line from the cation nucleus to the approximate center of the deformation density of the LEP; details are available elsewhere [9–16]. Its length ($|\boldsymbol{\Phi}_i|$) measures indirectly the deformation density of the LEP. Although this length is a useful tool, as it is dimensionless, it cannot be depicted graphically to link the asymmetry in the local coordination sphere to the LEP electron density. It is worth noting that the empirical BVS of an ion with LEP shows a linear correlation with $|\boldsymbol{\Phi}_i|$ [14, 17, 19].

In this study a combined experimental and theoretical approach was used to further explore the $\boldsymbol{\Phi}_i$, in particular to its relation with the electronic density isosurfaces within the unit cell of the crystals and with the formal BVS. The relationship between each particular structure and the LEP's stereochemical activity was also discussed taking into account the theoretical data of four structures ($La_2Al_4O_{9/10}$ and $La_2Mn_4O_{9/10}$) of which only $La_2Mn_4O_{10}$ is reported to have been synthesized [20]. La^{3+} ion does not possess LEPs but has a very similar ionic radius to that of Bi^{3+} ($r(La^{3+}) = 130$ pm and $r(Bi^{3+}) = 131$ pm for the octa-coordinated cations [21]). Hence, the effect of the crystal structures on the electronic distribution of a selected environment was addressed in terms of atomic or electronic arrangements.

2. Experimental

Mullite-type $Bi_2Al_4O_9$, $Bi_2Fe_4O_9$, and $Bi_2Mn_4O_{10}$ powder could be prepared using the glycerin method. Bismuth nitrate and the corresponding metal nitrate were mixed in the stoichiometric ratio of the cations. After adding glycerin as a solvent and reducing agent for the nitrate groups, the samples were heated in a three step process up to 1023 K to obtain the powder product. Further details of the powder synthesis procedure [8], the top seeded solution growth to grow larger $Bi_2Fe_4O_9$, and $Bi_2Mn_4O_{10}$ single crystals [22] and the respective structural investigations [23–25] are described elsewhere. Small $Bi_2Al_4O_9$ single crystals were grown using the synthesized powder together with an excess of four times the amount of Bi_2O_3. The intensively mixed educts were heated at 1423 K for 24 h, then slowly cooled to 1023 K and finally quenched to room-temperature. The remaining Bi_2O_3 was dissolved in 2 N HNO_3 in a repeated washing process. The finally obtained single-crystals were optically selected and the single-crystal X-ray diffraction data of a suitable one collected. A STOE IPDS1 single crystal diffractometer was used at ambient temperature collecting data in a phi range from $-6°$ to $360°$ in $1°$ steps exposing each frame for 2 minutes. The cube like crystal used for the data collection was cut out of a bigger plate like piece using a diamond wire saw. After the data collection the edges of this cube were measured and a numerical absorption correction was applied. This absorption correction was calculated with the STOE software X'Shape (STOE & Cie GmbH Darmstadt, Germany). Details of the data collection are given in Table 1. The positional parameters were refined using the Shelx program package [26] based on the data published by Niizeki and Wachi in 1968 [27]. The more accurate positional parameters of the crystal structure, anisotropic displacement parameters and some of the respective interatomic distances determined here are given in Tables 2 and 3, respectively.

Theoretical calculations were performed with the crystalline orbital program CRYSTAL09 [28, 29] employing the Hartree Fock – Density Functional Theory (HF – DFT) hybrid method PW1PW [30]. In previous studies it was found that hybrid functionals are more reliable for the description of oxides, in particular for transition metal oxides with open-shell ground states [31]. DFT studies have also proven reliability for the calculation of mullite-type compounds, such as the asymmetry of the bismuth coordination polyhedron and the stereochemical activity of the Bi LEP in $Bi_2Ga_4O_9$ [32].

Table 1. Crystal and data collection data of $Bi_2Al_4O_9$.

Empirical formula	$Bi_2Al_4O_9$
Formula weight/10^{-3} kg mol^{-1}	675.89
Space group	*Pbam* (55)
a/pm	773.85(5)
b/pm	812.21(4)
c/pm	570.70(4)
Volume/10^{-30} m^3	358.70(4)
Z	2
Temperature/K	298(2)
Crystal density/gcm^{-3}	6.257
Absorption coefficient/mm^{-1}	49.52
F(000)	586
Crystal dimension/μm	20(2) × 20(2) × 20(2)
Theta range MoK_α	3.86°–30.21°
Reflection range	$-10 \le h \le 10$, $-11 \le k \le 11$, $-\ 8 \le l \le\ \ 8$
Reflections collected/unique	7300/579
Merging residual	$R_i = 0.0613$
Refinement method/ Program	Full-matrix least-squares F^2/ Shelx [26]
Data/restraints/parameters	501/0/44
Goodness-of-fit	1.177
Final Residuals [$I > 2\sigma(I)$]	$R_1 = 0.0238$, $wR_2 = 0.0563$
CSD-No.[a]	xx–xxxxx[a]

a: Further details can be obtained at Fachinformationszentrum Karlsruhe http://www.fiz-karlsruhe.de

Table 3. $Bi_2Al_4O_9$ interatomic metal-oxygen distances shorter than 340 pm.

Atoms	Ligand	Count	Distances/pm
Bi1	O2	2×	213.5(5)
	O11	1×	213.8(6)
	O11	1×	241.8(6)
	O2	2×	290.6(5)
Al1	O12	2×	186.4(4)
	O11	2×	193.9(4)
	O2	2×	195.0(4)
Al2	O3	1×	172.2(2)
	O12	1×	178.0(7)
	O2	2×	180.1(5)
	O12	1×	300.0(6)

The studied structures were optimized using experimental crystallographic data as starting geometries. The optimized structure of $Bi_2Al_4O_9$ based on the refined parameters here was used as the starting point to model $Bi_2Mn_4O_9$, $La_2Al_4O_9$, and $La_2Mn_4O_9$, while that of $Bi_2Mn_4O_{10}$ [24] was used to model $Bi_2Al_4O_{10}$, $Bi_2Fe_4O_{10}$, $La_2Al_4O_{10}$, and $La_2Mn_4O_{10}$. All basis sets were taken from the CRYSTAL website database [33]. The Monkhorst-Pack shrinking factor was set to 4 after energy convergence, corresponding to 27 independent *k*-points in the irreducible part of the Brillouin zone. A very large integration grid with 75 radial points and 974 angular points was adopted for the numerical integration of the exchange-correlation energy. For $Bi_2Fe_4O_9$ a high-spin antiferromagnetic solution was chosen for the calculations [34]. For the rest of the compounds containing atoms with unpaired spins, the high-spin ferromagnetic solution was adopted [35, 36]. In all cases the antiferromagnetic configuration

Table 2. Atomic coordinates and displacement parameters of $Bi_2Al_4O_9$.

Atom	Wyckoff	Site symmetry	*x*	*Y*	*z*	U_{eq}
Bi1	4*g*	..*m*	0.32955(3)	0.16749(4)	0	0.0087(2)
Al1	4*e*	..2	0	0	0.2610(3)	0.0078(4)
Al2	4*h*	..*m*	0.1468(3)	0.3406(3)	$^1/_2$	0.0082(5)
O11	4*g*	..*m*	0.3578(8)	0.4293(7)	0	0.0090(11)
O12	4*h*	..*m*	0.3642(8)	0.4123(7)	$^1/_2$	0.0086(11)
O2	8*i*	1	0.1286(6)	0.2063(5)	0.2502(8)	0.0103(8)
O3	2*d*	..2/*m*	0	$^1/_2$	$^1/_2$	0.0181(16)

Anisotropic displacement parameters $\times 10^4$/pm^2

Atom	U_{11}	U_{22}	U_{33}	U_{12}	U_{13}	U_{23}
Bi1	0.0085(2)	0.0075(2)	0.0102(2)	−0.00031(9)	0	0
Al1	0.0080(9)	0.0086(9)	0.0069(9)	0.0005(8)	0	0
Al2	0.0093(11)	0.0074(11)	0.008(1)	−0.0044(8)	0	0
O11	0.008(3)	0.005(2)	0.014(3)	−0.001(2)	0	0
O12	0.010(3)	0.009(3)	0.006(2)	−0.002(2)	0	0
O2	0.0120(16)	0.0097(16)	0.009(2)	−0.0019(14)	0.003(2)	−0.001(2)
O3	0.020(4)	0.012(3)	0.023(4)	0.006(4)	0	0

was calculated yielding negligible differences of the LEP charge distribution with respect to the ferromagnetic configuration.

We suggest a new parameter, **Liebau Density Vector** (*LDV*) (*to honor F. Liebau who died too early in 2011 before all the important usages of his theory were known to people*), that describes the length of a vector directed from the nucleus of an atom (here bismuth or lanthanum) to the maximum charge density of the LEP. In comparison to the WLE parameter described in the previous section, the LDV is a vector of a finite length that can be represented graphically in real space for visual characterization, while the WLE parameter determines only a direction and a dimensionless value.

LDV has been calculated for each compound using charge density distributions of optimized structures. These charge density distributions were calculated with CRYSTAL09 using a three-dimensional grid with a resolution of 5 pm created with the XCrySDen program [37]. The outputs of these calculations were processed with a custom script written in the Python language so as to calculate the Liebau Density Vector. In order to distinguish the LEP from bonds and oxygen-centered electrons, only charge density within a 110 pm radius sphere centered on Bi/La nuclei was plotted, using the Wolfram Mathematica 8 program [38].

3. Results and discussion

The values which characterize the stereochemical activity of the bismuth LEP obtained by different approaches in this study are listed in Table 4. Four hypothetical structures in which bismuth was replaced by lanthanum (structures *VII–X*) have also been calculated. Except for small discrepancies, the experimental and theoretical values appear to be in good agreement. Experimental geometries can be satisfactorily reproduced with PW1PW; differences in lattice parameters and cell volumes between experimental and calculated geometries are less than 0.9% and 1.1%, respectively.

A larger Wang-Liebau eccentricity parameter (experimental: *E-WLE* and theoretical: *Th-WLE*) evidences a higher stereochemical activity of the LEP in $Bi_2M_4O_9$ mullite-types than that of $Bi_2M_4O_{10}$ compounds (compare, for instance, structures *I*, *II*, and *VI*). The free space between Bi atoms in the O9 structures is larger than that in the O10 structures (Fig. 1c). In the latter, an O−O pair has its center at a position that is occupied by only one O atom in the O9 structures (Fig. 1d). Thus a reduced space in the region amid Bi atoms may lead to a more homogenous electron distribution of the LEP. In Fig. 2a and b the distances from Bi atoms to the bridging O atoms are shown for the theoretically calculated structures of $Bi_2Al_4O_9$ and $Bi_2Mn_4O_{10}$. This value is around 30% shorter in the O10 compound.

Plots of charge density difference isosurfaces (with respect to the neutral atoms at the lattice sites) are an alternative and direct way to visualize the stereochemical activity of the LEPs. For the O9 structures, the LEP is clearly visible using an isovalue of 0.005 e/10^{-6} pm^3 (Fig. 2a), while a much smaller value (0.001 e/10^{-6} pm^3) has to be used for the O10 structures in order to identify their corresponding LEPs (Fig. 2b). Consequently a lower asymmetry of the charge distribution is found for O10 structures, in agreement with the Wang-Liebau approach. The proximity of the oxygen atoms in O10 structures also forces the LEP to change its direction. LEPs can therefore accommodate on the plane defined by both opposing Bi atoms and the bridging O atoms in O9 structures, while the lack of space in O10 structures forces the LEPs to be directed out of that plane (Fig. 2a and b).

Three-dimensional charge-density difference maps allow distinguishing the center of the LEPs clearly. The magnitudes of both the Wang-Liebau eccentricity vector and the Liebau Density vector are positive (see Table 4, structures *I* to *VI*), and their directions are almost parallel.

Table 4. Experimental Wang–Liebau eccentricity parameter (E-WLE), experimental bond valence sum (E-BVS), theoretical Wang–Liebau eccentricity parameter (Th-WLE), theoretical bond valence sum (Th-BVS), and theoretical Liebau density vector length (Th-LDV) for the bismuth or lanthanum atoms of the studied structures I to X.

		E-WLE/10^{-5}	E-BVS/v.u.	Th-WLE/10^{-5}	Th-BVS/v.u.	Th-LDV/pm
I.	$Bi_2Al_4O_9$	4.28	3.65	4.33	3.71	82.3 ± 4
II.	$Bi_2Fe_4O_9$	4.24	3.47	4.42	3.57	81.4 ± 4
III.	$Bi_2Mn_4O_9$[a]	–	–	4.92[c]	3.59[c]	81.7 ± 4[c]
				4.33[d]	3.71[d]	82.3 ± 4
IV.	$Bi_2Al_4O_{10}$[a,e]	–	–	3.26/3.00	5.88/3.73	§/69.3 ± 4
V.	$Bi_2Fe_4O_{10}$	–	–	1.41	3.55	60.4 ± 4
VI.	$Bi_2Mn_4O_{10}$	1.70	3.45	1.81	3.54	66.5 ± 4[b]
VII.	$La_2Al_4O_9$[a,e]	–	–	0.61/0.75	3.17/2.99	[b]/[b]
VIII.	$La_2Mn_4O_9$[a,e]	–	–	0.32/0.31	3.02/3.02	[b]/[b]
IX.	$La_2Al_4O_{10}$[a]	–	–	0.22	3.14	[b]
X.	$La_2Mn_4O_{10}$	–	–	0.10	3.33	[b]

a: Hypothetical, non-synthesized compounds. b: In these structures the LEP is stereochemically inactive and the point of maximum charge cannot be defined. c: These results correspond to a stationary point in the potential energy surface which is not a real minimum. d: These results are identical to the ones of structure *I* because they were obtained with a single point calculation using its geometry. e: The symmetry of these structures is lower than for all the rest, thus two types of bismuth or lanthanum atoms are found.

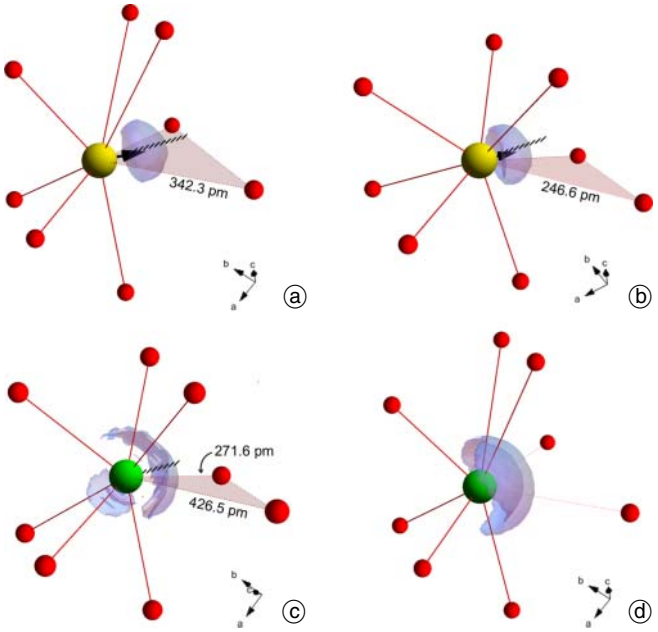

Fig. 2. Three-dimensional charge density difference isosurfaces and the theoretically calculated Bi coordination sphere. Yellow spheres represent bismuth atoms, green spheres represent lanthanum atoms, and red spheres represent oxygen atoms; arrows mark points of maximum charge (LDV), and dotted lines show the direction of Wang–Liebau eccentricity vectors. Only the eight closest oxygen atoms are shown. Distances to oxygen atoms bridging double tetrahedra are given, and shaded triangles indicate the planes containing them and bismuth atoms. (**a**) $Bi_2Al_4O_9$, isovalue: 0.005e/10^{-6} pm^3. (**b**) $Bi_2Mn_4O_{10}$, isovalue: 0.001 e/10^{-6} pm^3. (**c**) Optimized structure of $La_2Al_4O_9$, isovalue: 0.005 e/10^{-6} pm^3. (**d**) Isosurface for $La_2Al_4O_9$ with $Bi_2Al_4O_9$ geometry, isovalue: 0.005 e/10^{-6} pm^3.

The angle formed by both vector directions does not exceed 6 degrees in any of the $Bi_2M_4O_{9/10}$ structures (Fig. 2a and b, compare dotted lines and arrows representing the *Th-WLE* vector direction and the *Th-LDV* vector). In other words, even though the eccentricity parameter takes into account the LEP in an indirect fashion, DFT calculations show that this vector is indeed directed towards the point of maximum charge in the LEP, and that a larger magnitude is related to a more asymmetric charge distribution.

The effect of changing the cations at the M position on the stereochemical activity of the LEPs is rather small. This fact further shows that the stereochemical activity is mainly defined by the type of structure, *i.e.*, O9 or O10, which in turn determines the local Bi coordination.

The calculated Wang-Liebau eccentricity values (*Th-WLE*) in La containing compounds (structures *VII*–*X*) are small. But within the calculated values, they are found to be higher for the O9 compounds (structures *VII* and *VIII*) than for the O10 compounds. La^{3+} ions do not have a LEP, resulting in a homogeneous distribution of their electron density compared to Bi^{3+} mullite-type compounds. Nevertheless, charge density difference isosurfaces (Fig. 2c) show a small asymmetry for $La_2Al_4O_9$. A higher stereochemical activity is found for the case of the O9 compounds (structures *VII* and *VIII*). These facts can be explained by assuming that some bonds may be partially covalent and not fully ionic. The relatively large space existing in between two neighboring La atoms may allow the remaining electronic density to distribute in an inhomogeneous manner resulting in the calculated stereochemical activity. As is the case for $Bi_2M_4O_{9/10}$ structures, the stereochemical activity is determined by the local La coordination, and remains almost unchanged when Al is substituted by Mn (compare structures *VII* to *VIII*, and *IX* to *X*). In all four La structures the *LDV* could not be calculated, due to the poor charge asymmetry.

It must be noted that the optimized structures of $La_2Al_4O_9$ (Fig. 2c) and $La_2Mn_4O_9$ show an important distortion with a loss of symmetry with respect to the experimental and calculated structures of $Bi_2Al_4O_9$ and $Bi_2Fe_4O_9$ (results are not shown for the latter structure). In the distorted structures there are two types of lanthanum atoms, to which different Th-WLV and Th-BVS values can be assigned (Table 4). Furthermore, Fig. 2c shows that the distances between one of the lanthanum atoms and each of the two nearest bridging oxygen atoms are different (271.6 pm and 426.5 pm). These results suggest that the absence of a LEP in the lanthanum atom is detrimental to the stability of the structure.

In order to study the effect of exchanging bismuth for lanthanum atoms without geometry changes, single-point calculations of $La_2Al_4O_9$ were done using the $Bi_2Al_4O_9$ optimized geometry (without further optimization). The charge density difference isosurfaces (Fig. 2d) shows an asymmetric charge distribution for La, which ensures a larger value than that of the optimized structure (Fig. 2c). This is attributed to the larger void in the coordination sphere, a typical structural feature of $Bi_2Al_4O_9$ (compare distances from Bi to bridging O atoms in Fig. 2a and c).

Both the experimental bond valence sums (*E-BVS*) and theoretical bond valence sums (*Th-BVS*) of the stereochemically active moieties (Bi and La) showed a larger value (up to 0.71 valence units) than those of their formal valences of 3 v.u. (see Table 4). This appears to be in agreement with the results of Wang and Liebau [10] and Murshed *et al.* [17, 19], where positive deviations from the formal valence are shown to be caused by a high value of the eccentricity parameter. In compounds where bismuth was replaced with lanthanum (structures *VII* to *X*), the *Th-BVS* values are closer to the formal valence of 3, in correspondence with the absence of a LEP.

The relative stabilities of O9 and O10 structures are calculated according to the reactions given in Table 5.

In this study mullite-type O10 structures are only preferred when M is manganese, that is, $Bi_2Mn_4O_{10}$ and $La_2Mn_4O_{10}$ as shown in Table 5. In these compounds, M atoms are present in equal amounts as +3 and +4 ions. As Mn^{4+} is a stable ion, manganese containing com-

Table 5. Standard enthalpy changes (ΔH) at 298 K for the reactions involving the uptake of O_2 to obtain O10 structures from their analogous O9 compounds.

Reaction	ΔH/kJ mol^{-1}
$Bi_2Al_4O_9 + {}^1/_2\,O_2 \rightarrow Bi_2Al_4O_{10}$	249.3
$Bi_2Fe_4O_9 + {}^1/_2\,O_2 \rightarrow Bi_2Fe_4O_{10}$	57.9
$Bi_2Mn_4O_9 + {}^1/_2\,O_2 \rightarrow Bi_2Mn_4O_{10}$	−844.8
$La_2Al_4O_9 + {}^1/_2\,O_2 \rightarrow La_2Al_4O_{10}$	288.8
$La_2Mn_4O_9 + {}^1/_2\,O_2 \rightarrow La_2Mn_4O_{10}$	−905.9

pounds are able to adopt the O10 structure preferentially. On the other hand, as +4 is not a preferred valence of iron, and highly unfavorable to aluminum, bismuth and lanthanum, the O9 structures are consequently found to be more stable when M = Fe and/or Al. The results of Table 5 may explain why only O9 structures could be synthesized using iron or aluminum, whilst the O10 structures were obtained only with manganese [27]. It must be remarked that in mixed metal compounds the charges are conserved [23].

4. Conclusion

The experimentally determined structures of mullite-type $Bi_2Al_4O_9$, $Bi_2Fe_4O_9$, and $Bi_2Mn_4O_{10}$ were successfully reproduced using the hybrid HF/DFT approach PW1PW, allowing the computation of three-dimensional charge density isosurfaces to directly visualize the $6s^2$ Bi lone electron pair. The type of structure was found to be the main factor affecting the stereochemical activity of the LEP in $Bi_2M_4O_{9/10}$ compounds. The chemical nature of M (Al, Fe, or Mn) showed a negligible effect. A new term was coined as Liebau density vector (*LDV*) that describes the magnitude of the stereochemical activity of the lone electron pair of some ions, which further validates the Wang-Liebau eccentricity parameter ($|\boldsymbol{\Phi}_i|$). The *LDV* is therefore a proof that the purely geometrically defined Wang-Liebau vector indeed points towards the maximum electron density of the LEP, a key result of this work.

The geometry optimization of $La_2Al_4O_9$ (where lanthanum (III) cations do not have LEPs) showed a distortion of the local La coordination sphere compared to that of Bi in $Bi_2Al_4O_9$, suggesting a plausible structural stability factor introduced by the magnitude of $LDV/|\Phi_i|$. The fact that relative stabilities between O9 and O10 structures are correctly predicted further validates the application of hybrid HF/DFT methods to these compounds

Acknowledgements. We gratefully acknowledge the Agencia Nacional de Promoción Científica y Tecnológica (ANPCYT), Argentina, for the financial support for the project PICT-2683. CBM is member of the research staff of Consejo Nacional de Investigaciones Científicas y Técnicas (CONICET, Argentina). MC is grateful to CONICET for the postgraduate scholarship. We also like to thank the Deutsche Forschungsgemeinschaft (DFG) for the financial support through the mullite-LEP project GE1981/4–1. TMG especially likes to thank the DFG for the support in the Heisenberg program (GE1981/3-1)

References

[1] J. B. Goodenough, A. Manthiram, P. Paranthaman, Y. S. Zhen, *Solid State Ionics* **1992**, *52*, 105–109.
[2] R. X. Fischer, H. Schneider, *The Mullite-Type Family of Crystal Structures*, ed. H. Schneider and S. Komarneni, Mullite Wiley-VCH Weinheim, 2005, vol. 1–46, 128–140.
[3] I. Abrahams, A. J. Bush, G. E. Hawkes, T. Nunes, *J. Solid State Chem.* **1999**, *147*, 631–636.
[4] S. Ohmann, P. Fielitz, L. Dörrer, G. Borchardt, Th. M. Gesing, R. X. Fischer, C. H. Rüscher, J.-Ch. Buhl, K.-D. Becker, H. Schneider, *Solid State Ionics* **2012**, *211*, 46–50.
[5] J. Schreuer, M. Burianek, M. Mühlberg, B. Winkler, D. J. Wilson, H. Schneider, *J. Phys.: Cond. Matter* **2006**, *18*, 10977–10988.
[6] Th. M. Gesing, M. Schowalter, C. Weidenthaler, M. M. Murshed, G. Nénert, M. Curti, C. B. Mendive, A. Rosenauer, J.-Ch. Buhl, H. Schneider, R. X. Fischer, *J. Mater. Chem.* **2012**, *22*, 18814–18823.
[7] S. Zha, J. Cheng, Y. Liu, X. Liu and G. Meng, *Solid State Ionics* **2003**, *156*, 197–200.
[8] Th. M. Gesing, R. X. Fischer, M. Burianek, M. Mühlberg, T. Debnath, C. H. Rüscher, J. Ottinger, J.-Ch. Buhl, H. Schneider, *J. Eur. Ceram. Soc.* **2011**, *31*, 3055–3062.
[9] X. Wang, F. Liebau, *Z. Kristallogr.* **1996**, *211*, 437–439.
[10] X. Wang, F. Liebau, *Acta Crystallogr.* **1996**, *B52*, 7–15.
[11] X. Wang, F. Liebau, *Mater. Res. Soc. Symp. Proc.* **2005**, *848*, 345–350.
[12] F. Liebau, X. Wang, *Z. Kristallogr.* **2005**, *220*, 589–591.
[13] X. Wang, F. Liebau, *Acta Crystallogr.* **2007**, *B63*, 216–228.
[14] X. Wang, F. Liebau, *Acta Crystallogr.* **2009**, *B65*, 96–98.
[15] F. Liebau, X. Wang, W. Liebau, *Chem. Eur. J.* **2009**, *15*, 2728–2737.
[16] F. Liebau, X. Wang, *Z. Kristallogr.* **2005**, *220*, 589–591.
[17] M. M. Murshed, A. Rusen, R. X. Fischer, Th. M. Gesing, *Mater. Res. Bull.* **2012**, *47*, 1323–1330.
[18] I. D. Brown, The Chemical Bond in Inorganic Chemistry, The Bond Valence Model, Oxford University Press, 2002
[19] M. M. Murshed, R. X. Fischer, Th. M. Gesing, *Z. Kristallogr.* **2012**, *227*, 580–584.
[20] J. A. Alonso, M. T. Casais, M. J. Martínez-Lope, J. L. Martínez, M. T. Fernández-Díaz, *J. Phys.: Condens. Matter* **1997**, *9*, 8515–8526.
[21] R. D. Shannon, *Acta Crystallogr.* **1976**, *A32*, 751–767.
[22] M. Burianek, M. Mühlberg, M. Woll, M. Schmücker, Th. M. Gesing, H. Schneider, *Cryst. Res. Technol.* **2009**, *44(10)*, 1156–1162.
[23] H. Schneider, R. X. Fischer, Th. M. Gesing, J. Schreuer, M. Mühlberg, *Int. J. Mat. Res.* **2012**, *103*, 422–429.
[24] M. Burianek, Th. F. Krenzel, M. Schmittner, J. Schreuer, R. X. Fischer, M. Mühlberg, G. Nénert, H. Schneider, Th. M. Gesing, *Int. J. Mat. Res.* **2012**, *103*, 449–455.
[25] M. M. Murshed, G. Nènert, M. Burianek, L. Robben, M. Mühlberg, H. Schneider, R. X. Fischer, Th. M. Gesing, *J. Solid State Chem.* **2013**, *197*, 370–378.
[26] G. M. Sheldrick, A short history of SHELX. *Acta Crystallogr.* **2008**, *A64*, 112–122.
[27] N. Niizeki, M. Wachi, The crystal structure of $Bi_2Mn_4O_{10}$, $Bi_2Al_4O_9$, and $Bi_2Fe_4O_9$. *Z. Kristallogr.* **1968**, *127*, 173–187.
[28] R. Dovesi, R. Orlando, B. Civalleri, C. Roetti, V. R. Saunders, C. M. Zicovich-Wilson, *Z. Kristallogr.* **2005**, *220*, 571–573.
[29] R. Dovesi, V. R. Saunders, C. Roetti, R. Orlando, C. M. Zicovich-Wilson, F. Pascale, B. Civalleri, K. Doll, N. M. Harrison, I. J. Bush, P. D'Arco and M. Llunell, CRYSTAL09, 2009, CRYSTAL09 User's Manual. University of Torino, Torino.
[30] T. Bredow, A. R. Gerson, *Phys. Rev. B* **2000**, *61*, 5194–5201.
[31] M. Marsman, J. Paier, A. Stroppa, G. Kresse, *J. Phys. Condens. Matter* **2008**, *20*, 064201.
[32] J. Schreuer, M. Burianek, M. Muehlberg, B. Winkler, D. Wilson, H. Schneider *J. Phys.: Condens. Matter* **2006**, *18*, 10977–10988.
[33] http://www.crystal.unito.it/Basis_Sets.
[34] N. Shamir, G. Gurewitz, *Acta Crystallogr.* **1978**, *A34*, 662–666.
[35] Z. R. Kann, J. T. Auletta, E. W. Hearn, S.-U. Weber, K.-D. Becker, H. Schneider, M. W. Lufaso, *J. Solid State Chem.* **2012**, *185*, 62–71.
[36] S.-U. Weber, Th. M. Gesing, G. Eckold, R. X. Fischer, F.-J. Litterst, K.-D. Becker, *submitted*.
[37] A. Kokalj, *Comp. Mater. Sci.* **2003**, *28*, 155–168.
[38] Wolfram Research, Inc., Mathematica, Version 8.0, Champaign, IL (2010).